

# Analysis of PD control of mechanical systems with dynamic backlash

<sup>†</sup>M. T. Mata-Jiménez <sup>\*</sup>, <sup>†</sup>B. Brogliato and <sup>‡</sup>A. Goswami

<sup>†</sup> Laboratoire d'Automatique de Grenoble, UMR CNRS-INPG 5528  
Domaine Universitaire, B.P. 46, 38402 St. Martin D'Hères, France

e-mail: mata, brogli@lag.ensieg.inpg.fr

<sup>‡</sup>INRIA Rhône-Alpes

ZIRST, 655 avenue de l'Europe, 38330 Montbonnot St. Martin, France

e-mail: ambarish.goswami@inrialpes.fr

## Abstract

This paper is devoted to the analysis and control of a simple rigid body mechanical system with dynamic backlash. Contrary to most of the existing work in control literature we explicitly treat all the dynamic and non-linear characteristics of this system. We show that appropriate gains in a PD control scheme can be selected such that the closed-loop system is locally stable around a desired symmetric periodic orbit. Two cases are analyzed: the collocated and the non-collocated controllers. It is shown that both schemes are quite similar, although the non-collocated case yields, as expected, smaller existence and stability regions. This work finds potential application in several areas including the control of kinematic chains with joint clearance and vibro-impact systems.

## 1 Introduction

Backlash is one of the most important non-linearities that taxes the control strategies implemented in the industrial machines and degrades the overall performance of the machines. It causes delays, oscillations, and consequently gives rise to inaccuracies in the position and velocity of the machine. In extreme cases, backlash related effects can help set in chaos in the system thereby making it completely intractable from the point of view of the controller.

Backlash commonly occurs in bearings, gears and impact dampers. It arises from unavoidable manufacturing tolerances or are often deliberately incorporated in the system to accommodate thermal expansion [2]. Fig 1 presents the sketch of a simple system with backlash which uses a rigid body contact/impact model.

---

<sup>\*</sup>Supported by CONACYT-México

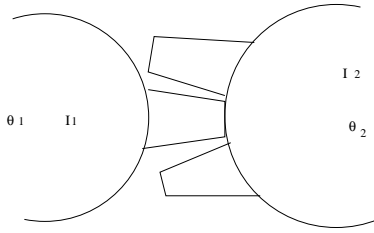


Figure 1: System with backlash

[11] analyzed the problem and proposed to model backlash as a hysteresis function between the output and input positions of the system. This is a geometric model in which the system input is  $\theta_1$  and the output is  $\theta_2$ . Given that the dynamic effects of the collisions are not taken into account in this model, it cannot describe the real dynamics of the system in Fig. 1. This backlash model does not approximate the real physical system in Fig. 1 as it makes the un-physical assumptions that the shocks are purely inelastic and that the ratio of the inertias of the two interacting masses,  $\frac{I_1}{I_2}$ , is zero. The control strategy mainly consists of a discontinuous input which makes sure that the two gears are *always* in contact. This means that the gears never stay free in the clearance and make instantaneous position jumps from one contact to the other. This is an idealized behavior only possible for an inertia-less system.

In [1] the authors investigate the control of a system with dynamic backlash. With respect to Fig. 1 their control model considers the torque  $\tau_1$  as the input and the position  $\theta_2$  as the output. In their control model, the effect of impact of the gears on the dynamics of the first gear (in Fig. 1) is considered as a disturbance. In order to explore the limit cycle behavior of the system they base their study on the describing function techniques. Their study is carried out by means of numerical simulations only.

[8] formulated the dynamic equations of motion for an impact pair including compliance at the contact. In his model,  $\tau$  is the input and  $\theta_2$  the output. It is assumed that  $I_1 = 0$ , i.e. the system is an inertia free elastic shaft system with backlash. Contrarily to [11] their linear control input uses a low gain when the system evolves inside the clearance. [8] justifies the choice of the compliant contact/impact model by citing laboratory experimental results.

Several other backlash models have been proposed and studied in the mechanical engineering literature [10] and, in particular, in relationship with the so-called impact damper. [2, 6] studied the dynamic response of simplified rigid-body impacting systems. They showed the existence of complex dynamics including different types of periodic trajectories, bifurcations, and chaotic motion.

In this work the impact damper (see Fig. 2) is used as a simplified model of backlash for feedback control purposes incorporating the dynamical effects of impacts. We use a rigid body model which is justified by typical numerical values of  $10^7$ N/m for the contact/impact stiffness and a contact damping of 10Ns/m between metals that have been reported in the literature. For instance, consider a

simple system that consists of a mass striking a rigid wall. If the contact/impact process is modeled by a spring with stiffness  $k = 10^{10}\text{N/m}$ , simple calculations [4] yield an impact duration of  $10^{-3}$  s. for  $m=1\text{kg}$ . We wish to underline here that in contrast to the models of [11] and [8] we consider the torque  $\tau_1$  as the input and the angular position  $\theta_2$  as the output. In the linear backlash model as shown in the Fig. 2 this corresponds to  $U$  and  $x_1$ , respectively. In our opinion this is the most practical model for control purposes in a machine with clearance. Our study finds potential application in the control of robot manipulators whose performance may be degraded because of the presence of clearance in the joints.

In this paper we apply PD control strategy to this system and identify the realizable stable periodic solutions. Our objective here is to treat the control parameters, the gains of a PD control scheme in the same footing as the physical parameters (such as the mass and the clearance length) of the system and study the controller performance as a function of these gains. This we believe is a novel approach. We show that similar to the effect of the change in physical parameters on the system dynamics, the control parameters can also qualitatively change the system dynamics. The study involves highly nonlinear equations and we eventually rely on simulation results. Thus, although we cannot analytically guarantee the existence of any stable periodic orbit, in practice, we find one within a few trials.

## 2 Controlled impact-damper model

A schematic diagram of the mechanical system under consideration is shown in Fig. 2, which consists of a secondary mass  $m_2$  subject to an external control input  $U$  and a primary mass,  $m_1$ , which is constrained to move in a slot inside the mass  $m_2$ . The supposed frictionless motion of  $m_1$  is instigated by collisions with  $m_2$  which occur intermittently because of the clearance  $2L$ . The play comes from the size of the slot in  $m_2$  being larger than the size of  $m_1$ . Due to the absence of friction, the velocity of  $m_1$  remains constant between two consecutive impacts. The physical contacts may repeat many times, leading to a finite or infinite number of collisions.

This idealized model is called an *impact pair*. It is a simplified version of many typical mechanical systems with clearances. Because of its simplicity, it has been used frequently as a basic model for the study of mechanical systems with clearances [2, 10, 4] and references therein. Although it is an approximate model, it exhibits the typical behavior found in such systems and has an extremely rich dynamics.

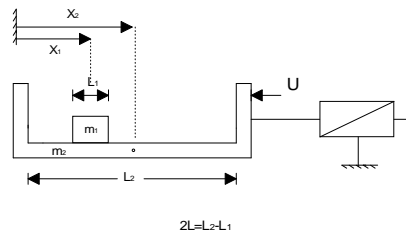


Figure 2: Physical model

The equations governing the motion between two successive impacts are:

$$\begin{aligned} m_1 \ddot{x}_1 &= 0 \\ m_2 \ddot{x}_2 &= U \end{aligned} \quad \text{for } |x_1 - x_2| < L \quad (1)$$

All impacts are supposed, reasonably for metals, to be instantaneous and described by a coefficient of restitution,  $e$ , representing the energy lost during collision [3].

From the definition of the coefficient of restitution, the linear momentum conservation and considering that the positions of the masses are not changed during the impact, the following relations can be obtained,

$$\begin{pmatrix} x_1(t_k^+) \\ x_2(t_k^+) \\ \dot{x}_1(t_k^+) \\ \dot{x}_2(t_k^+) \end{pmatrix} = \begin{pmatrix} 1 & 0 & 0 & 0 \\ 0 & 1 & 0 & 0 \\ 0 & 0 & \frac{\mu-e}{1+\mu} & \frac{(1+e)}{1+\mu} \\ 0 & 0 & \frac{(1+e)\mu}{1+\mu} & \frac{1-\mu e}{1+\mu} \end{pmatrix} \begin{pmatrix} x_1(t_k^-) \\ x_2(t_k^-) \\ \dot{x}_1(t_k^-) \\ \dot{x}_2(t_k^-) \end{pmatrix} \rightarrow X(t_k^+) = \mathcal{E}X(t_k^-) \quad (2)$$

where  $t_k^+$  and  $t_k^-$  denote the velocities just after and just before the  $k^{th}$  impact and  $\mu = \frac{m_1}{m_2}$  is called the mass ratio.

Let us consider the case where  $L = 0$ , i.e. the clearance is zero and  $x = x_1 = x_2$  (there are no impacts). Then this second order system is easily controlled via a  $PD$  controller of the form

$$U = m_2 \ddot{x}_d - k_v \dot{\tilde{x}} - k_p \tilde{x}, \quad k_p > 0, k_v > 0 \quad (3)$$

with  $\tilde{x} = x - x_d$  and  $x_d$  is a desired trajectory. This control is applied only on  $m_2$ .

In the following we shall choose  $x_d$  as a cosine function,

$$x_d = x_m \cos \omega t \quad (4)$$

so that  $U$  can be rewritten as

$$U = -k_v \dot{x} - k_p x + \beta \cos(\omega t + \zeta) \quad (5)$$

with

$$\beta \cos(\omega t + \zeta) = m_2 \ddot{x}_d + k_v \dot{x}_d + k_p x_d \quad (6)$$

The closed-loop behavior of the controlled system is given by,

$$m_2 \ddot{x}_2 = -k_v \dot{x} - k_p x + \beta \cos(\omega t + \zeta) \quad (7)$$

For the system with  $L \neq 0$ , this control is effective only between impacts. Since the collisions are considered instantaneous, this control has no effect during the impacts. However the impacts influence the evolution of  $m_2$  and  $m_1$ . It is important to observe that the motion of  $m_1$  can only be indirectly controlled via collisions. For the feedback purposes  $x$  can be chosen as  $x_2$  or  $x_1$ . The first case is the collocated control and the second is called the non-collocated control. The closed loop behavior of the system can be rewritten as a set of first-order equations:

$$\begin{aligned}
\dot{x}_1 &= y_1 \\
\dot{y}_1 &= 0 \\
\dot{x}_2 &= y_2 \\
m_2 \dot{y}_2 &= -k_v y - k_p x + \beta \cos(\omega t + \zeta)
\end{aligned} \tag{8}$$

where  $x_1$  and  $y_1$  are the displacement and velocity of the primary mass,  $x_2$  and  $y_2$  are the displacement and velocity of the secondary mass, and  $(x, y) = (x_1, y_1)$  for the non-located case or  $(x, y) = (x_2, y_2)$  for the collocated case .

Note that the system contains eight parameters  $(k_p, k_v, x_m, \omega, \mu, e, L, m_2)$ , but for this study, all the parameters will be kept fixed except the gains  $k_p, k_v$  which are varied in order to investigate their effects on the dynamics and control of the system.

### 3 Determination of periodic solutions

The construction of the periodic trajectories created by the control law is based on the observation that the equations governing the closed loop system between collisions are linear; thus explicit solutions can be obtained. These solutions are concatenated at the instant of impact with an impact rule to obtain a complete solution.

A periodic solution of order  $n$  will mean a solution which has a period  $n$  times the period of the control input  $T = \frac{2\pi}{\omega}$  (where  $n$  is an integer). In the system there exist many different types of periodic solutions of order  $n$ . However, in order to simplify the algebraic calculations only those periodic solutions which have a single impact with each of the boundaries during a single cycle will be taken into account (this is the simplest solution possible), referred to as *simple periodic solutions*. Finding the general solution is at best extremely difficult and [2] demonstrate that the exact closed form solutions are possible only when the number of collisions per period is equal to two.

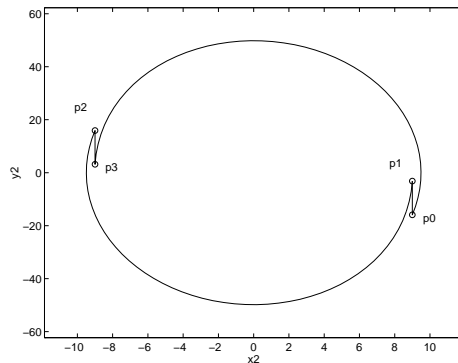


Figure 3: Diagram of the flow of the secondary mass in the phase plane

To build the periodic trajectory only the secondary mass is considered. To find a simple periodic solution, it is assumed that the oscillator starts at the boundary

$x_2 = x_{20}$  with initial velocity  $y_{20}$  as shown in Fig. 3 (corresponding to  $p_0$ ). A complete cycle is as follows: The secondary mass starts at  $p_0$  and immediately jumps to  $p_1$  via a virtual coefficient of restitution  $R$  which will be defined later. The subsequent motion is governed by the differential equation and the system moves until it reaches the boundary  $x_2 = x_{22}$  at  $p_2$ , at which point it again jumps, this time to  $p_3$ . The mass continues to move until it reaches the boundary  $x_2 = x_{40}$  at  $p_4$ . If  $p_4 = p_0$ , then the orbit is periodic.

The method proposed is slightly different from the method presented in [6]. The main difference is the introduction of a virtual coefficient of restitution  $R$  to accommodate the discontinuous velocities at a collision and the effect of the primary mass. In using  $R$  the periodicity can be related only to the secondary mass, the dynamics of the primary mass being taken into account by the coefficient  $R$ . In the next section we will obtain an expression for  $R$ .

Within the simple periodic solutions, there are two different types of motion: symmetric solutions in which the projection of the trajectory is symmetric with respect to the origin and the masses spend an equal time between two consecutive impacts, and asymmetric solutions which do not satisfy this property. In the following, only the symmetric periodic trajectories will be considered.

### 3.1 Symmetric solutions

The values of  $k_p$  and  $k_v$  such that there exists a simple symmetric periodic solution are searched. Because of symmetry, only one half of the cycle needs to be considered for the study. The symmetry conditions require that  $x_{22} = -x_{20}$ , and the time elapsed between two consecutive shocks is  $\Delta = \frac{nT}{2}$ . The system should satisfy also the following conditions:  $y_{12} = -y_{10}$ ,  $y_{22} = -y_{20}$ ,  $x_{22} = -x_{20}$  and  $\sin(\omega t_0 + \zeta) = -\sin(\omega t_0 + \zeta + n\pi)$ . The last condition shows that  $n$  must be odd.

Following the method suggested above, the periodic solutions are computed at steady-state. In other words, the cycle is built assuming the existence of a periodic solution with the symmetry characteristics and evaluating the solutions at the collision instant. For steady-state motion with two impacts per cycle, if one impact occurs at  $t = t_0$ , the next impact will occur at  $t = t_0 + \frac{nT}{2}$ . The velocity of the primary mass remains constant between two consecutive shocks. Consequently, the velocity of  $m_1$  during  $(t_0, t_1)$  is equal to its velocity at  $t_0^+$ . Hence  $y_{10}$  is equal to the ratio of the distance traveled and the time elapsed between the two impacts of the cycle,

$$y_{10} = 2(L + x_{20})\frac{\omega}{n\pi} = 2x_{10}\frac{\omega}{n\pi} \quad (9)$$

The equations (2) can be rearranged to obtain the velocities of the secondary mass before and after the collision as a function of the parameters of the system and the position of the impact,

$$y_{20} = \left(\frac{e - 2\mu - 1}{1 + e}\right) y_{10} \quad (10)$$

$$y_{21} = \left(\frac{e + 2e\mu - 1}{1 + e}\right) y_{10} \quad (11)$$

A virtual coefficient of restitution  $R$  can be obtained which gives the velocity of the secondary mass after an impact as a function of its velocity before the collision and the physical parameters of the system,

$$y_{21} = Ry_{20}, \quad R = \frac{\epsilon + 2\epsilon\mu - 1}{\epsilon - 2\mu - 1} \quad (12)$$

Now the analysis can be referred only to the secondary mass given that the effect of the primary mass is considered by the coefficient  $R$ .

Conditions for the existence of a symmetric periodic solution are given by (only in terms of the secondary mass)

$$x_{22} = x_2 \left( t_0 + \frac{nT}{2}; x_{20}, Ry_{20}, t_0 \right) = -x_{20} \quad (13)$$

$$y_{22} = y_2 \left( t_0 + \frac{nT}{2}; x_{20}, Ry_{20}, t_0 \right) = -y_{20} \quad (14)$$

Because the conditions are given in the collision instant, the analysis is equal for both the collocated and non-collocated cases. Only the solutions of the linear equations between collisions are different.

### 3.2 Existence conditions

If we define  $\varphi = t \bmod T$ , the equations (13) and (14) involve  $\cos(\omega\varphi_0)$  and  $\sin(\omega\varphi_0)$  linearly, and can be solved. Solving the equations for sine and cosine provides the equations (15) and (16).

$$\sin(\omega\varphi_0) = sn(x_{20}, Ry_{20}, \varphi_0) \quad (15)$$

$$\cos(\omega\varphi_0) = cs(x_{20}, Ry_{20}, \varphi_0) \quad (16)$$

$$sn^2(x_{20}, Ry_{20}, \varphi_0) + cs^2(x_{20}, Ry_{20}, \varphi_0) = 1 \quad (17)$$

The expressions  $sn$  and  $cs$  depend on the physical parameters. They are different for the collocated and the non-collocated cases.

It is worth noting that contrary to what is stated in [6] this condition is not sufficient to guarantee the existence of a periodic trajectory. Indeed the existence condition of the impact motion excludes the possibility of the occurrence of an additional impact during the time interval between the periodic impacts [9, 5]. This can be expressed via so-called *viability conditions* as

$$|x_1 - x_2| < L \quad \text{for} \quad t_0 < t < t_0 + \frac{nT}{2} \quad (18)$$

The existence boundary of the given impact region must satisfy the following conditions,

$$|x_1 - x_2| = L \quad y_1 - y_2 = 0 \quad (19)$$

The values of  $k_p$  and  $k_v$  can be obtained only numerically since the process of obtaining them requires finding the roots of transcendental equations.

The necessary and sufficient conditions for the existence of the periodic trajectories are in (17) and (18). Notice that from (17),  $x_m$  can be expressed as

$$x_m = x_m(x_{20}, Ry_{20}, \varphi_0) \quad (20)$$

Hence condition (17) can be replaced by the condition that  $x_m$  in (20) exists. Thus  $x_m$  can be eliminated as a parameter.

## 4 Stability of periodic solutions

In this section we will study the stability of periodic motions induced by the control law described in the previous section. Periodic orbits correspond to fixed points of the Poincaré map. The stability analysis of these orbits consists of computing the Jacobian matrix  $DP$  of the Poincaré map at the periodic orbits and finding the eigenvalues. A periodic motion is stable if and only if the moduli of all the eigenvalues of  $DP$  are less than unity.

### 4.1 The Poincaré map

One of the most basic tool for studying the stability of periodic orbits is the *Poincaré map*. The principal idea of the Poincaré map is to replace the continuous  $n$ th-order system by an  $(n - 1)$ th-order discrete system. In practice, the Poincaré map is derived by setting up a hypersurface of  $(n - 1)$  dimension in a state space. If the section is chosen properly, the states intersect it repeatedly. The Poincaré map is defined by the evolution of the intersections. One replaces the study of the flow of the differential equation by the difference equation defining the evolution. In terms of the Poincaré map, the orbital stability is reduced to the problem of the stability of a fixed point of the map, which is characterized by the eigenvalues of the map linearized about the fixed point.

In order to obtain a section to generate the Poincaré map  $P$ , one must have some knowledge of the geometrical structure of the phase space of the problem. For the system considered in this paper, it is possible to obtain a section relying on the insight of the system behavior. That is, the collisions take place when the two masses come in contact and the bodies move apart from each other after an impact. If the collision is repeated many times, the evolution of the system will be given by the system state evolution at the impact instants. This is a natural choice of the section given the nature of the system. It is important to observe that the discrete formulation of the Poincaré map enables one to eliminate the problem of discontinuities due to impacts.

To simplify the notation  $z_1 = x_2$ ,  $z_2 = y_2$ ,  $z_3 = x_1 - x_2$  and  $z_4 = y_1 - y_2$  will be used. In this system the hypersurface defined by the collisions is chosen as:

$$\Sigma = \{(z_1, z_2, z_3, z_4, \varphi) | z_3 = L, z_4 > 0\} \quad (21)$$

Because of the discontinuities, the Poincaré map must be constructed by composition of four simple mappings,

$$P = P_{43} \circ P_{32} \circ P_{21} \circ P_{10} \quad (22)$$

where  $P_{43}$  and  $P_{21}$  is the contribution of the flight between constraints and  $P_{32}$  and  $P_{10}$  are the impact discontinuities. The system dynamics are given by the evolution equation:

$$\begin{pmatrix} \varphi_4 \\ z_{14} \\ z_{24} \\ z_{44} \end{pmatrix} = P \begin{pmatrix} \varphi_0 \\ z_{10} \\ z_{20} \\ z_{40} \end{pmatrix} \quad (23)$$

Notice that  $P$  is known only in implicit form. Indeed the solution of the time elapsed between impacts ( $\tau_1$  and  $\tau_2$ ) requires finding the roots of transcendental equations. The Poincaré map defined by this section is not the usual stroboscopic one which samples the phase space once per period of the excitation. Instead, an *impact map* is used, the phase space is sampled before the impacts.

## 4.2 Analysis for symmetric solutions

The Poincaré map defined above is given only in implicit form, because to obtain an explicit expression for the flight time is impossible. However, the behavior of the system can be characterized by the *local* stability of the fixed points. The periodic solutions correspond to fixed points of the Poincaré map.

In order to determine the stability of a periodic solution emanating from  $(\varphi_0, z_{10}, z_{20}, z_{40})$ , the Jacobian matrix of the Poincaré map  $P$  at  $(\varphi_0, z_{10}, z_{20}, z_{40})$  must be calculated. This derivative is obtained using implicit differentiation. The calculation of  $DP$  is carried out by considering the dynamics of small perturbations of the periodic solutions. Given the nature of the map only the sensitivity matrix  $DP$  is known.

The computation of  $DP$  must be decomposed into four parts to consider the contribution of each mapping:

$$DP(\varphi_0, z_{10}, z_{20}, z_{40}) = \frac{\partial(\varphi_4, z_{14}, z_{24}, z_{44})}{\partial(\varphi_0, z_{10}, z_{20}, z_{40})} = DP_{43} DP_{32} DP_{21} DP_{10} \quad (24)$$

where

$$DP_{ij} = \frac{\partial(\varphi_i, z_{1i}, z_{2i}, z_{4i})}{\partial(\varphi_j, z_{1j}, z_{2j}, z_{4j})} \quad (25)$$

$DP_{10}$  and  $DP_{32}$  representing the evaluation of the velocity discontinuities are given by the impact rule. In (24)  $DP_{21}$  and  $DP_{43}$  come from the free flight. In this mapping the evolution of the perturbation from the post-collision state to the next pre-collision state is governed by the differential equation. The variables  $\varphi_2$ ,  $z_{12}$ ,  $z_{22}$  and  $z_{42}$  are related to  $\varphi_1$ ,  $z_{11}$ ,  $z_{21}$  and  $z_{41}$  by

$$\begin{aligned} g &= z_{32}(\varphi_2; \varphi_1, z_{11}, z_{21}, z_{41}) = -L \\ f_1 &= z_{12}(\varphi_2; \varphi_1, z_{11}, z_{21}, z_{41}) \\ f_2 &= z_{22}(\varphi_2; \varphi_1, z_{11}, z_{21}, z_{41}) \\ f_3 &= z_{42}(\varphi_2; \varphi_1, z_{11}, z_{21}, z_{41}) \end{aligned} \quad (26)$$

The stability of the periodic solution for the linearized system is determined by the eigenvalues of the perturbation matrix  $DP$ . The solution is asymptotically stable if and only if all the eigenvalues have a module less than the unity. The considered fixed points must be hyperbolic to eliminate the degenerated solutions and the possibility of the existence of bifurcations.

The eigenvalues of the matrix  $DP$  are given by

$$|\lambda I - DP| = 0 \quad (27)$$

The resulting equation is a fourth order polynomial, the stability limits will be given when the moduli of one of its solutions take the value 1.

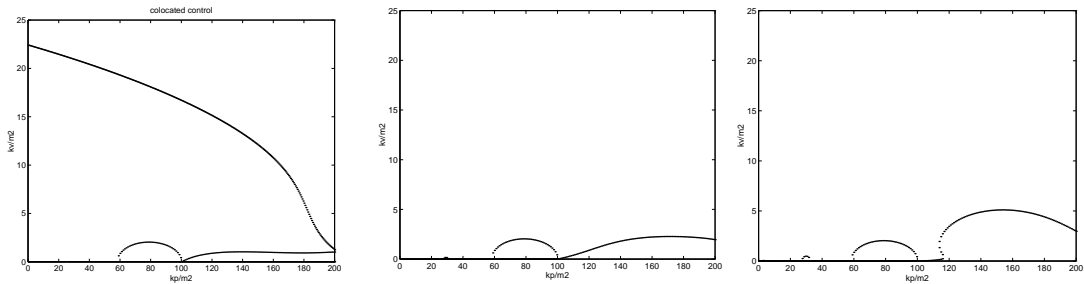


Figure 4: Superposition of the existence and stability regions as a function of the gains  $(k_p, k_v)$  for the collocated control ( $\mu = 0.1, \gamma = 0.75, n = 1, \omega = 5, e = (0.1, 0.5, 0.9)$ )

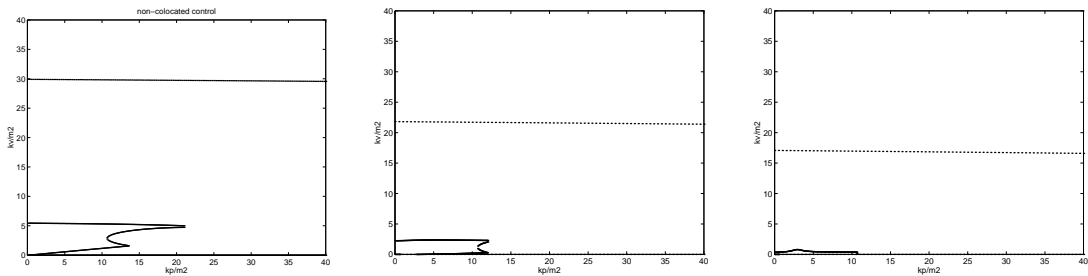


Figure 5: Superposition of the existence and stability regions as a function of the gains  $(k_p, k_v)$  for the non-collocated control ( $\mu = 0.1, \gamma = 0.75, n = 1, \omega = 5, e = (0.1, 0.5, 0.9)$ )

Figures 4 and 5 show the range of gains  $k_p, k_v$  for which the desired symmetric trajectory of the primary mass (corresponding to the parameters values in the captions) exists and is stable. The shaded portions represent the intersection of the stability and existence regions.

## 5 Concluding comments

We can make the following conclusions from figures 4, 5, 6, 7

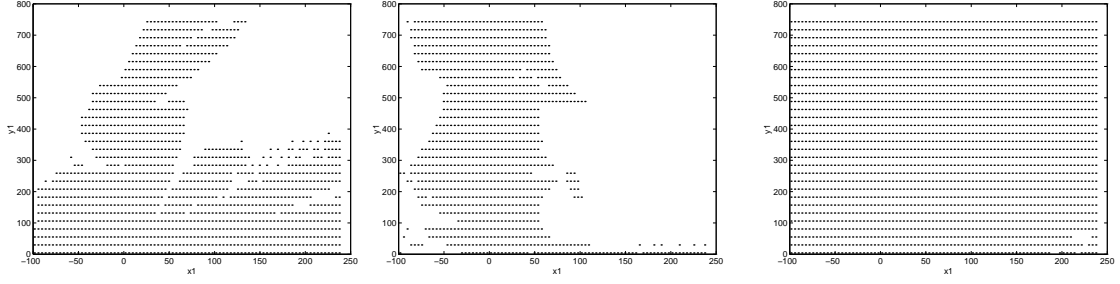


Figure 6: Basins of attraction for the collocated control ( $\mu = 0.1, \gamma = 0.75, n = 1, \omega = 5, k_p = 10, k_v = 20, e = (0.1, 0.5, 0.9)$ )

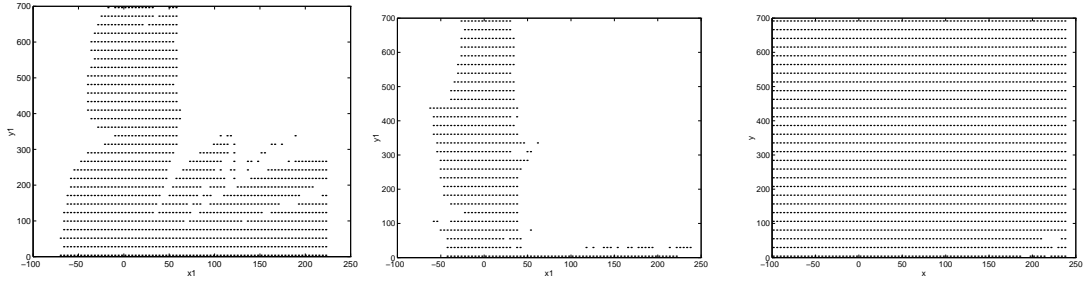


Figure 7: Basins of attraction for the non-collocated control ( $\mu = 0.1, \gamma = 0.75, n = 1, \omega = 5, k_p = 10, k_v = 20, e = (0.1, 0.5, 0.9)$ )

- The existence and stability regions are much smaller for the non-collocated case than for the collocated one, as expected.
- For the non-collocated case the region of existence and stability decreases with increasing  $e$ . It is the inverse for the collocated case.
- The range of admissible gains corresponding to the chosen stable periodic trajectory is large for the collocated case.
- It is possible to obtain similar figures for other parameters. Recall that the set of figures corresponds to a particular desired trajectory for the primary mass. However notice that to each couple  $(k_p, k_v)$  correspond a different secondary mass trajectory.
- It is of interest, in particular, to study the influence of  $\mu$  on the system behavior. The two extreme cases  $\mu = 0$  and  $\mu = \infty$  can be analytically investigated. For  $\mu \rightarrow \infty$  one can see that  $y_1$  becomes continuous even at impacts, while the relative velocity is strictly positive after impacts. Therefore the control has no effect on the motion of the primary mass. This shows that the existence region tends to decrease with increasing  $\mu$ . On the contrary as  $\mu$  tends to zero, the effects of the primary mass on the secondary mass become negligible. Intuitively, this facilitates the control since the non-linearities in the secondary mass dynamics vanish. The influence of  $L$  (that is  $\gamma$ ) also deserves future attention.

- It is clear that the  $PD$  control provides only local stability. It is therefore of interest to study a control strategy which can enlarge the basins of attraction. A hybrid control strategy which fulfills this objective has been proposed in [7].
- In order to obtain the basins of attraction in figures 6 and 7, we have considered that a given trajectory converges towards the desired one if  $(x_1^* - x_1)^2 + (y_1^* - y_1)^2 + (y_2^* - y_2)^2 + (\varphi^* - \varphi)^2 < 0.001$  after 1500 iterations of the Poincaré map, i.e. 3000 collisions.
- Notice that the real basins of attraction contain the depicted ones, since the convergence criterion eliminates trajectories with a too slow transient. Moreover the depicted figures represent a section of the real basins of attraction in the  $(x_1, y_1, y_2, \varphi) = (x_1, y_1, y_2^*, \varphi^*)$ -subspace.
- Although the existence and stability regions for the non-colocated case are much smaller than for the colocated one, the basins of attraction have a similar size in both cases. However in practice the uncertainties on the physical parameters will be an obstacle to the implementation of the non-colocated control, due to the smallness of the admissible feedback gains regions.

## References

- [1] A. Azenha and J. A. Tenreiro Machado. Variable structure control of systems with nonlinear friction and dynamic backlash. In *13th World Congress of IFAC*, pages 515–520, San Francisco, USA, July 1996.
- [2] C. N. Bapat, N. Popplewell, and K. McLachlan. Stable periodic motions of an impact-pair. *Journal of Sound and Vibration*, 87(1):19–40, 1983.
- [3] R. M. Brach. *Mechanical impact dynamics*. John Wiley, New York, 1991.
- [4] B. Brogliato. *Nonsmooth impact mechanics. Models, dynamics and control*. Number 220 in LNCIS. Springer Verlag, 1996.
- [5] M. S. Heiman, P. J. Sherman, and K. Bajaj. On the dynamics and stability of an inclined impact pair. *Journal of Sound and Vibration*, 114(3):535–547, 1987.
- [6] G. X. Li, R. H. Rand, and F. C. Moon. Bifurcations and chaos in a forced zero-stiffness impact oscillator. *Journal of Non-linear Mechanics*, 25(4):417–432, 1990.
- [7] M. T. Mata-Jimenez, B. Brogliato, and A. Goswami. On the control of mechanical systems with dynamic backlash. In *IEEE Conference on Decision and Control*, December 1997.
- [8] M. Nordin. *Uncertain systems with backlash: Modeling, identification and Synthesis*. PhD thesis, Royal Institute of Technology, Stockholm, Sweden, May 1993.
- [9] F. Peterka and J. Vacik. Transition to chaotic motion in mechanical systems with impacts. *Journal of Sound and Vibration*, 154(1):95–115, 1992.
- [10] Y. Stepanenko and T. S. Sankar. Vibro-impact analysis of control systems with mechanical clearance and its application to robotic actuators. *Journal of Dynamic Systems, Measurement, and Control*, 108:9–16, March 1986.
- [11] G. Tao and P. V. Kokotovic. Adaptive control of systems with backlash. *Automatica*, 29(2):323–335, 1993.